

Correlation dimension and phase space contraction via extreme value theory

Davide Faranda*

LSCE-IPSL, CEA Saclay l'Orme des Merisiers,

CNRS UMR 8212 CEA-CNRS-UVSQ,

Université Paris-Saclay, 91191 Gif-sur-Yvette, France

Sandro Vaienti†

Université de Toulon, CNRS, and Centre de Physique Théorique, UMR 7332, 83957 La Garde, France

We show how to obtain theoretical and numerical estimates of correlation dimension and phase space contraction by using the extreme value theory. Maxima of suitable observables sampled along the trajectory of a chaotic dynamical system converge asymptotically to classical extreme value laws where: i) the inverse of the scale parameter gives the correlation dimension, ii) the extremal index is associated to the rate of phase space contraction for backward iteration, which in dimension 1 and 2 is closely related to the positive Lyapunov exponent and in higher dimensions is related to the metric entropy. We call it the Dynamical Extremal Index. Numerical estimates are straightforward to obtain as they imply just a simple fit to an univariate distribution. The estimates of the phase space contraction index is particularly robust even with relatively short time series.

1. INTRODUCTION

Since its introduction in the eighties by Grassberger and Procaccia [1, 2], the correlation dimension (CD) has been used as a powerful indicator for the description of the fractal structure of invariant sets in dynamical systems. Similarly, the Lyapunov exponents and the entropy [3, 4] provide an indication of the relevant time scales associated to the dynamics and the predictability horizon of the system. Given the importance of these quantities, there exists an increasing body of literature on how to estimate CD, Lyapunov exponents and entropy. It has been shown that reliable estimates of CD can be obtained with relatively short time series [5]. Instead, the computations of Lyapunov exponents and entropy are still challenging because the existing methodologies require as input additional parameters as the dimension of the phase space and the relevant time scale of the dynamics (e.g. the decorrelation time). Calculations are then limited to the top Lyapunov exponent and the reliability of estimates from time series of experimental phenomena is often questioned [6]. We defer the reader to the monographs [7], [8] and to the articles [9], [10] for recent advancements on the various statistical tools to investigate nonlinear time series.

In the past decade the extreme value theory (EVT), has been used to characterize and made prediction on the evolution of chaotic systems [11, 12]. Within this framework, it is possible to obtain dynamical properties in phase space (fractal dimension or stability) by exploiting the limiting theorems of the extreme value theory. The main idea is to replace the stochastic processes used in the statistical framework, with a trajectory of a chaotic dynamical system. Then one studies the convergence of maxima of suitable observables to the classical extreme value laws. The parameters of the EVT provide, in the asymptotic limits, estimates of dynamical properties of the system.

*Electronic address: davide.faranda@cea.fr; Also at: London Mathematical Laboratory, 14 Buckingham Street, London, WC2N 6DF, UK

†Electronic address: vaienti@cpt.univ-mrs.fr

This elegant connection between EVT and the dynamical properties of chaotic systems is rich not only from a theoretical but also from a numerical perspective. Indeed the estimates of local properties obtained with EVT do not require the introduction of additional parameters and they are easy to implement numerically. They have been used to get insights on the dynamical behavior of atmospheric flows in [13–15]. In [16], it has been shown that the numerical algorithm based on EVT provide reliable estimates of the dimension of high dimensional systems up to phase spaces with thousands of dimension. It is therefore desirable to estimate other key dynamical quantities in the EVT framework.

The purpose of this communication is to show that the correlation dimension and the EVT are intimately related, in particular the CD arises by studying the distribution of the maxima of a new suitable observable evaluated along the orbit of a chaotic system. Moreover, an exponent of the limit law, the extremal index, is related to the positive Lyapunov exponent in dimension two and to the metric entropy in higher dimensions. The idea of the relationship between EVT and CD comes from a previous work [17] where we used extreme value theory to detect and quantify the onset of synchronization in coupled map lattices. The relationship between the extremal index and the Lyapunov exponent and the entropy is new and is particularly striking for maps with piecewise constant jacobian. In the general case we guess a formula which is pretty well satisfied on the examples. We also explain how that index is related to the local dimensions and the joint effects, dimension and phase space contraction, should be taken in mind when the index is computed. In the rest of the paper we will name it as the DEI, the *dynamical extremal index*. We want to point out that our DEI is a very well defined quantity which can be used as a new indicator for the sensitivity associated to local hyperbolicity. We will present the theoretical results in the next section: some of those results can be obtained by generalizing the techniques introduced in [17]; we will also address the need to develop a more appropriate theory of EVT for diffeomorphisms in higher dimensions. We will then provide several examples of classical conceptual dynamical systems; these systems are low-dimensional ones. We will then argue and discuss the implications of our results on higher dimensional systems and the possibility to apply them to more general time series. As an example we will consider here the atmospheric circulation and we will provide estimates of the correlation dimension and of the extremal index for 110 years of sea-level pressure fields over the North Atlantic issued from the ERA 20CM reanalysis dataset.

2. THEORETICAL RESULTS

Let us suppose (M, μ, T) is a dynamical systems given by a map T acting on the metric compact space M with distance $d(\cdot, \cdot)$ and preserving the Borel measure μ . Usually M will be a compact subset of some \mathbb{R}^n and d a distance equivalent to the standard one. Then take the *direct product*

$$(M \times M, \mu \times \mu, T \times T),$$

and denote with $(x, y) \in M \times M$, a couple of point in the cartesian product $(M \times M)$. We then introduce the observable

$$\psi(x, y) = -\log d(x, y), \quad (2.1)$$

and consider the process $\{\psi \circ (T^j \times T^j)\}_{j \geq 0}$, and the maximum of the sequence:

$$\mathcal{M}_n(x, y) = \max\{\psi(x, y), \psi(Tx, Ty), \dots, \psi(T^{n-1}x, T^{n-1}y)\} \quad (2.2)$$

and finally its distribution $\mathbb{P}(\mathcal{M}_n \leq u_n)$, where $\mathbb{P} = \mu \times \mu$ is the underlying probability and u_n is a suitable scaling function tending to infinity and which we are going to define. Suppose that for a given positive number τ we can find a sequence of numbers u_n such that

$$n\mathbb{P}(\psi \geq u_n) \rightarrow \tau, \quad n \rightarrow \infty. \quad (2.3)$$

Then we say that the process $\{\psi \circ (T^j \times T^j)\}_{j \geq 0}$ satisfies an extreme value law of Gumbel's type if there is a number $\theta \in (0, 1]$, the *extremal index*, such that

$$\mathbb{P}(\mathcal{M}_n \leq u_n) \rightarrow e^{-\theta\tau}, \quad n \rightarrow \infty. \quad (2.4)$$

We now introduce the diagonal neighborhood S_n in the product space: $S_n = \{(x, y), d(x, y) \leq e^{-u_n}\}$; by substituting the expression of ψ in the left hand side of (2.3), we have

$$\mathbb{P}(\psi \geq u_n) = \mathbb{P}((x, y) \in S_n) = \int_M \mu(B(x, e^{-u_n})) d\mu(x), \quad (2.5)$$

where $B(x, a)$ denotes the ball of radius a centered at x [46]. For ergodic measures it has been proved in [18] that the quantity

$$\frac{1}{N^2} \sum_{\substack{i,j=1 \\ i \neq j}}^{N^2} H(r - d(T^i x, T^j x)), \quad (2.6)$$

where H denotes the Heaviside function, converges to

$$\int_M \mu(B(x, r)) d\mu(x) \quad (2.7)$$

when $n \rightarrow \infty$ for μ -almost every x and uniformly in r on any bounded interval $[0, R], R > 0$. The quantity in (2.7) scales like r^{D_2} and the exponent D_2 is called the *correlation dimension* and it characterizes the fractal structure of the support of μ . This scaling was firstly proposed in [1] associated to the sum (2.6); a more formal, from the mathematical point of view, definition is given in [19], sect. 17, and references therein [47]. By injecting successively into (2.5) and (2.3) we have therefore that for large n :

$$u_n \sim \frac{-\log \tau}{D_2} + \frac{\log n}{D_2} := \frac{y}{a_n} + b_n. \quad (2.8)$$

where $\tau = e^{-y}$, $a_n = D_2$ and $b_n = \frac{\log n}{D_2}$. We now remember that for numerical purposes, distribution functions like $\mathbb{P}(\mathcal{M}_n \leq y)$ are modelled, for n sufficiently large, by the so-called *generalized extreme value (GEV)* distribution which is a function depending upon three parameters $\xi \in \mathbb{R}, \mu \in \mathbb{R}, \sigma > 0$: $\text{GEV}(y; \mu, \sigma, \xi) = \exp \left\{ - \left[1 + \xi \left(\frac{y-\mu}{\sigma} \right) \right]^{-1/\xi} \right\}$.

The parameter ξ is called the tail index; when it is 0, the GEV corresponds to the Gumbel type. The parameter μ is called the location parameter and σ is the scale parameter: for n large the scaling constant a_n is close to σ^{-1} and b_n is close to μ . Therefore if we could detect a limit law of Gumbel's type with suitable normalizing parameters a_n and b_n , we could catch the correlation dimension. Such a technique was previously used but with a different observable, and it allowed to get the so-called *information dimension* $D_1(x)$, that is another fractal dimension which gives the scaling of the measure of a ball around a given point x , see [20] and references therein. Although the information dimension depends on the point x , its value is the same for almost all the choices of x with respect to the invariant measure and such an averaged value, simply D_1 , is larger or equal to D_2 , see [21] for an account on the different fractal dimensions. In particular if we denote with d_H the Hausdorff dimension, we have $D_2 \leq D_1 \leq d_H$. Before showing our numerical simulations for the computation of the CD, let us argue how we get a Gumbel's type asymptotic distribution with an extremal index θ of dynamical meaning. We consider first one-dimensional dynamical systems generated by uniformly expanding maps with an invariant set which could be a Cantor set and equipped with Gibbs measures. These measures are characterized by a potential φ of type $\varphi(x) = -\beta \log |T'(x)|$, where $\beta \in \mathbb{R}$. These measures, denoted as μ_β , are given by $h_\beta \nu_\beta$ where the density h_β and the *conformal* measure ν_β are respectively the eigenfunctions of the transfer operator (Perron-Fröbenius) and of its dual, both with eigenvalue $\lambda_\beta = e^{P(\beta)}$, being $P(\beta)$ the topological pressure; we defer to the monograph [22] for an introduction to thermodynamic formalism. The

conformal measure verifies the property

$$\nu_\beta(TA) = \lambda_\beta \int_A e^{-\varphi} d\nu_\beta, \quad (2.9)$$

where T is one-to-one over the measurable set A . A good knowledge of the transfer operator allows us to use the spectral approach to EVT firstly proposed by Keller [23]; see also our paper [17] for a detailed presentation, the only difference being that we now work with the direct product map $\bar{T} = T \times T$ and the maximal, isolated, eigenvalue of the direct product operator, λ_β^2 , is generally different from 1. With these precautions and following the proofs in the aforementioned papers, it is easy to check that the dynamical extremal index θ is given by

$$\theta = \frac{1 - \lambda_\beta^{-2} q_0}{\lambda_\beta^2} \quad (2.10)$$

where q_0 is given by [24]

$$q_0 = \lim_{n \rightarrow \infty} \frac{\mathbb{P}_\beta(S_n \cap \bar{T}^{-1}S_n)}{\mathbb{P}_\beta(S_n)}, \quad (2.11)$$

provided the limit exists, and where now $\mathbb{P}_\beta = \mu_\beta \times \mu_\beta$. The computation of q_0 proceeds as in [17] with a substantial difference: the nature of the conformal measure (2.9) does not imply necessarily that the ratio $\frac{\nu_\beta(B(Tx, r))}{\nu_\beta(B(x, r))}$ is constant, which happened when the conformal measure was Lebesgue. This difficulty could be partially overcome by supposing that the potential is constant, otherwise we could bound q_0 from above and below with (close) approximations of the potential. Assuming the latter is constant and equal to $\bar{\varphi}$ and also that the density h_β does not vary too much we get that q_0 is of order $e^{\bar{\varphi}}$ and therefore

$$\theta \sim \frac{1 - \lambda_\beta^{-2} e^{\bar{\varphi}}}{\lambda_\beta^2}. \quad (2.12)$$

It is worth mentioning that whenever the conformal measure is Lebesgue ($\beta = 1$), the above computation can be made rigorous as in Proposition (5.3) in [17] and it gives

$$\theta = 1 - \frac{\int_M \frac{h^2(x)}{|T'(x)|} dx}{\int_M h^2(x) dx}, \quad (2.13)$$

where h is the density of the invariant measure: we defer to our paper [17] for the assumptions on the system which permit to get such a result. Notice that by introducing the invariant measure $\mu = hdm$ we could identically write

$$\theta = 1 - \frac{\int_M h(x) e^{-\log|T'(x)|} d\mu(x)}{\int_M h(x) d\mu(x)}. \quad (2.14)$$

If the derivative does not change too much we get $\theta \sim 1 - e^{-\Lambda_\mu}$, where Λ_μ is the positive Lyapunov exponent of the measure μ . Alternatively, if the density h could be considered constant we can bound (2.14) by Jensen's inequality as

$$\theta \sim 1 - \int_M \frac{1}{|T'(x)|} d\mu(x) \leq 1 - e^{-\int_M \log|T'(x)| d\mu(x)} = 1 - e^{-\Lambda_\mu}.$$

In both cases the DEI θ is related to the positive Lyapunov exponent: this analogy will be pursued in the next section.

2.1. Attractors and high dimensional systems

For invertible maps generating attractors endowed with the SRB measure, the computation of the dynamical extremal index is less straightforward; we should stress at this regard that a spectral theory of extreme value for

(invertible) uniformly hyperbolic maps is still missing. Suppose we take an hyperbolic diffeomorphisms T preserving the ergodic SRB measure \mathcal{L} . Then the quantity q_0 in (2.11) becomes

$$q_0 = \lim_{n \rightarrow \infty} \frac{\int d\mathcal{L}(x) \int \mathbf{1}_{S_n}(x, T^{-1}y) \mathbf{1}_{S_n}(Tx, y) d\mathcal{L}(y)}{\int d\mathcal{L}(x) \int \mathbf{1}_{S_n}(x, y) d\mathcal{L}(y)}. \quad (2.15)$$

When we iterate backward the points $y \in B(Tx, e^{-u_n})$, we should keep only those whose preimage is at a distance at most e^{-u_n} from x . Those preimages form a set $Q(x)$ which is obtained by squeezing the ball $B(Tx, e^{-u_n})$ along the unstable manifolds. Let us suppose that the tangent expanding subspace $\Sigma_u(Tx)$ at x has dimension d . Then the measure of $Q(x)$, and therefore by the forward invariance of the measure, of its image in $B(Tx, e^{-u_n})$ will be of order $|\det(DT(x)|_u)|^{-1} \mathcal{L}(B(Tx, e^{-u_n}))$, where $DT(x)|_u$ is the derivative of T restricted to $\Sigma_u(x)$. We remember in fact that the conditional SRB measure on the unstable manifolds is smooth. This immediately gives q_0 of order

$$q_0 \sim \frac{\int d\mathcal{L}(x) |\det(DT(x)|_u)|^{-1} \mathcal{L}(B(Tx, e^{-u_n}))}{\int d\mathcal{L}(x) \mathcal{L}(B(Tx, e^{-u_n}))} \quad (2.16)$$

We see that q_0 contains information about the dimension through the scaling of the denominator, see (2.7); we are now interested in the contribution of the other term in the numerator. At this regard we first remind that for the SRB measure we have the Pesin's formula [25]:

$$\int d\mathcal{L}(x) |\det(DT(x)|_u)| = \sum_{j=1}^d \Lambda_j^+ = h_{\mathcal{L}},$$

where the Λ_j^+ are the positive Lyapunov exponents which we took with multiplicity one, and $h_{\mathcal{L}}$ is the metric entropy of the SRB measure. At this point we proceed with two assumptions as we did at the end of the previous section. Let us first assume that the derivative along the unstable subspaces does not change too much; therefore we could estimate the DEI as

$$\theta \sim 1 - e^{-h_{\mathcal{L}}}. \quad (2.17)$$

For $d = 1$ we can replace the entropy with the unique positive Lyapunov exponent $\Lambda_{\mathcal{L}}$; in the following we will simply write it as Λ_+ .

The other alternative explores the fact that for these system and for \mathcal{L} -almost all points x we have, by Young's theorem [26], that $\lim_{r \rightarrow 0} \frac{\log \mathcal{L}(B(x, r))}{\log r} = D_1$, where D_1 is the information dimension. Hence we could guess that $\mathcal{L}(B(x, e^{-u_n})) \sim e^{-u_n D_1}$ and therefore forget about the dependence on the variable x . This is in general false since the multiplicative factor in the previous scaling could depend on x and in fact when we integrate $\mathcal{L}(B(x, e^{-u_n}))$ we get D_2 which could be different from D_1 . If we suppose that the dependence on x of the prefactors is negligible, which in substance means that we are considering an homogenous fractal invariant set with $D_1 \sim D_2$, then we have for the DEI:

$$\theta \sim 1 - \int d\mathcal{L} |\det(DT(x)|_u)|^{-1} \leq 1 - e^{-\int d\mathcal{L} |\det(DT(x)|_u)|} = 1 - e^{-h_{\mathcal{L}}}, \quad (2.18)$$

where the derivative is not supposed now to be constant and we use again Jensen's inequality to establish the upper bound.

Those two approximations are very crude; we are in fact either neglecting the contributions of the prefactors in the local scaling of the balls in (2.16), or we did not take into account the geometric factors when the ball $B(Tx, e^{-u_n})$ is squeezed at a distance e^{-u_n} from x . Moreover the variation of the derivative, especially sensible in the non-uniformly hyperbolic setting, could give large differences in the determination of the DEI, as we experienced for instance for the Hénon map, see below. The preceding relation is pretty well satisfied for maps with one-dimensional unstable subspace and (piecewise) constant jacobian, like the Baker transformation, the Lozi map and the solenoid. For the

algebraic automorphism of the torus (cat's map), a simple argument allows us to improve the previous rate just by taking into account the geometric factors. Surprisingly relation (2.18) is pretty well satisfied in the example below of the generalized Hénon maps, where the unstable subspace has dimension larger than one, which means we have more than one positive Lyapunov exponent. In conclusion our index θ catch in a satisfactory way the entropy, and the deviation from that are due to the variation of the derivative and the local scaling of balls in (2.16). The latter effects are difficult to compute analytically; instead the DEI θ is relatively easy to compute numerically and it furnishes a new indicator for the local instability in chaotic systems: the next section will illustrate that with several examples.

3. EXAMPLES AND NUMERICAL COMPUTATIONS

The numerical computations of correlation dimensions are done with the following algorithmic procedure (see appendix A for a MATLAB numerical code):

1. l pairs of trajectories $T^i x$ and $T^i y$ each consisting of $i = 1, 2, \dots$ iterations of the maps are produced.
2. For each pair, the observable $\psi(T^i x, T^i y)$ is computed.
3. The maxima are extracted in m block of length n such that $s = mn$. A block is defined as a set of m subsequent observations of the trajectory.
4. The maxima are fitted to the GEV distribution with a maximal likelihood estimator.
5. For each l we extract $D_2 = 1/\sigma$ and the extremal index by using the Suveges method [27] which requires to sample all the clusters beyond the quantile \tilde{s} . Each cluster represent the set of subsequent observations that fall beyond \tilde{s} . We recall that this happens when the trajectories become close to each other.
6. For each map, the estimate of D_2 is obtained by averaging over the l realizations of the maps. The associated uncertainty is the standard deviation of the sample.

The stability of the results is checked against different l, n, m . Although the quality slightly depend of the map, we found that reliable estimates of D_2 and θ can be obtain with $l > 10$, $n > 10^5$, $m > 300$ and $0.97 < \tilde{s} < 0.999$ except where specified.

3.1. Low dimensional maps

We begin the numerical computations with several examples on low dimensional maps. A summary of the results for all maps analysed is reported in Table 1 for $l = 100$, $n = 10^6$, $m = 1000$ and $\tilde{s} = 0.99$. They include several 1D and 2D maps that we will briefly describe in the sequel.

- Let us begin with the Bernoulli Shift map $T(x) = 3x \bmod 1$. For this system $D_2 = 1$ and $\theta = 1 - 1/3 = 2/3$. The numerical estimates are coherent with the theoretical values since $D_2 = 1.00 \pm 0.02$ and $\theta = 0.668 \pm 0.004$.
- We now consider the Gauss map $T(x) = \frac{1}{x} \bmod 1$ defined on the unit interval. Although, strictly speaking, this map does not fit the assumptions in [17], we still try formula (2.13), since for the Gauss map the density is explicit and reads $h(x) = \frac{1}{\log 2} \frac{1}{1+x}$. The integral in (2.13) can be easily computed and gives $\theta = 4 \log(2) - 2 \sim 0.77$, whereas D_2 is expected to be 1. The numerical estimates give indeed $D_2 = 1.00 \pm 0.03$ and $\theta = 0.773 \pm 0.005$.
- Returning to a map with constant slope 3, we now look at the transformation generating the classical ternary Cantor set. This map belongs to the class of the conformal repellers, see for instance [28]. In order to compute

numerically the GEV function, one should access the invariant Cantor set, which is of zero Lebesgue measure. We need therefore to use the backward iterates of the map (otherwise almost all the forward orbits will fall into the holes), and the measures allowing us to compute the time averages are the so-called *balanced measures*, given suitable weights to the preimages of the map: see our article [29], section 3.2.2 for a description of such measures. For the ternary Cantor set and choosing equal weights $1/2$ for the two preimages, it is easy to check that such a balanced measure coincides with the Gibbs measure with $\beta = \log 2 / \log 3$ which is the Hausdorff dimension of the invariant set. The measure μ_{d_H} is called *uniform*, see [21], Sect.3. The potential φ will be equal to $-\log 2$ and $\lambda = 1$, since by Bowen's formula $P(d_H) = 0$. Therefore for the ternary Cantor set we get a DEI equal to 0.5 which is perfectly confirmed by the numerical simulations. In fact $D_2 = 0.64 \pm 0.01$ and $\theta = 0.502 \pm 0.005$

- For the Lozi map : $x_{n+1} = a|x_n| + y_n + 1, y_{n+1} = bx_n, a = 1.7, b = 0.5, \Lambda_+$ is of order $0,47$ [30], which gives, with our approximation, a DEI of order $\theta = 0.37$. Previous numerical computations for D_2 gave $D_2 \sim 1.38$, [31]. Instead the GEV computations indeed $D_2 = 1.39 \pm 0.11$ and $\theta = 0.37 \pm 0.01$.
- For the Hénon map $x_{n+1} = ax_n^2 + y_n + 1, y_{n+1} = bx_n, a = 1.4, b = 0.3, \Lambda_+$ is of order $0,42$ [30], which gives, with our approximation, a DEI of order $\theta = 0.34$. Previous numerical computations for D_2 gave $D_2 \sim 1.22$, [31]. The GEV computations give $D_2 = 1.24 \pm 0.11$ but $\theta = 0.43 \pm 0.01$. The discrepancy of the DEI estimate does not get any better with the increase of \tilde{s} or n . As said before, we do not expect θ to coincide with the estimate 0.34 due to the variation of the derivative and the non-uniform hyperbolicity of the map.
- Let us consider the cat's map with the associated matrix $\begin{pmatrix} 1 & 1 \\ 1 & 2 \end{pmatrix}$. The stable and unstable manifolds for such a map are orthogonal, so we could suppose that the preimage of the ball $B(Tx, e^{-u_n})$ will intersect the ball $B(x, e^{-u_n})$ in a rectangle $R(x)$ centered at x and with the shortest side of length $(\lambda_+)^{-1}e^{-u_n}$, where $\lambda_+ = \frac{3+\sqrt{5}}{2}$ is the eigenvalue larger than 1 corresponding to the unstable direction. An elementary calculation shows immediately that $q_0 \sim \mathcal{L}(R(x))/\mathcal{L}(B(x, e^{-u_n}))$ is approximately given by $\frac{4}{\pi}(\lambda_+)^{-1}$ which gives an extremal index as 0.51 . Previous numerical computations for D_2 gave $D_2 \sim 1.987$, [31]. The numerical computation with the GEV function gives $D_2 = 2.00 \pm 0.06$ and $\theta = 0.552 \pm 0.005$. In order to investigate the discrepancy with our theoretical estimate, we raised the quantile from $\tilde{s} = 0.99$ to $\tilde{s} = 0.999$, i.e. we select more extreme clusters. The estimates for this case are $\theta = 0.54 \pm 0.02$, more compatible with the theoretical one. Finally, if we consider longer trajectories ($n = 10^7$ iterates) with an even higher quantile ($\tilde{s} = 0.9999$), we get $\theta = 0.53 \pm 0.06$, which is even closer to the theoretical guess.
- The baker's map is defined on the unit square $[0, 1] \times [0, 1]$ iteratively for $n \geq 1$, by

$$x_{n+1} = \begin{cases} \gamma_a x_n, & \text{for } y_n < \alpha \\ \frac{1}{2} + \gamma_b x_n, & \text{for } y_n > \alpha \end{cases}$$

$$y_{n+1} = \begin{cases} \frac{1}{\alpha} y_n, & \text{for } y_n < \alpha \\ \frac{1}{1-\alpha} (y_n - \alpha) + \gamma_b x_n, & \text{for } y_n > \alpha \end{cases}$$

The positive Lyapunov exponent is given by [21], eq. 5.14:

$$\Lambda_+ = \alpha \log \frac{1}{\alpha} + (1 - \alpha) \log \frac{1}{1 - \alpha}$$

With the value $\alpha = 1/3, \gamma_a = 1/5, \gamma_b = 1/4$, we get $\Lambda_+ \sim 0,64$ which gives, with our approximation, an extremal index of order $0,47$. In the paper [21], eq. 5.18, we gave an implicit formula expressing D_2 as a

function of α and with respect to the SRB measure. For $\alpha = 1/3$, this estimate reads $D_2 \simeq 1.41$. The GEV estimates give $D_2 = 1.46 \pm 0.02$ and $\theta = 0.49 \pm 0.02$.

- We next consider an attractor embedded in \mathbb{R}^3 , the so-called solenoid. The space M will be now the direct product of the circle S^1 parametrized by $\{t : 0 \leq t < 1\}$ with the disk $D = \{(u, v) \in \mathbb{R}^2 : u^2 + v^2 \leq 1\}$. The space M will be therefore the solid torus $M = S^1 \times D$. The map T will be defined by

$$T(t, u, v) = (2t(\text{mod}1), au + \frac{1}{2} \cos(2\pi t), av + \frac{1}{2} \sin(2\pi t)), \quad 0 < a < \frac{1}{2}. \quad (3.19)$$

It is well known that the original torus is successively wrapped into itself and the limiting intersection is an attractor with not integer dimension. The attractor will be foliated by one-dimensional unstable manifolds, while each meridional disk is a two-dimensional stable manifold each of which intersecting the attractor over a Cantor set. The Lyapunov exponents are

$$\Lambda_- = \log a < 0, \quad \Lambda_+ = \log 2,$$

while the Hausdorff dimension d_H is given by the formula [32]

$$d_H = 1 + \frac{\log 2}{-\log a}.$$

The numerical computations for the solenoid provide a further test of the validity of the numerical algorithm. For $a = 1/3$, $d_H \simeq 1.6309$. Indeed the numerical estimates give $D_2 = 1.64 \pm 0.04$. For $a = 1/4$, $d_H = 1.5$ while the numerical estimates give $D_2 = 1.52 \pm 0.03$. The value of θ is independent on a since it is linked only to Λ_+ . Theoretically, we expect $\theta = 0.5$ and numerically we get $\theta = 0.51 \pm 0.01$ for both the ensemble of realizations.

3.2. High dimensional generalized Hénon maps

We now analyze the generalized Hénon maps defined in [33] and further analyzed in [34]. They are defined as:

$$x_{n+1}(1) = ax_n(d-1)^2 - bx_n(d) \quad x_{n+1}(i) = x_n(i-1) \quad (3.20)$$

When the parameter $a = 1.76$ the number of positive Lyapunov exponents is $d-1$; we could therefore test our relation (2.18) by computing the entropy $h_{\mathcal{L}}$ as the sum of positive Lyapunov exponents (see Tab. 2 in [34]) for a given d . We also perform the computation of the dimension D_2 and compare it to the Kaplan-Yorke dimension D_{KY} given in [34]. The good agreement between our numerical results confirm the validity of Eq. 2.18 with the caveat that an exact correspondence cannot be derived for the geometric factor that stretch balls in phase space in different dimensions.

3.3. Application to atmospheric data

We now consider an application to atmospheric data. The purpose of this application is to show the applicability of the technique on real data and that it provides results that have a coherent interpretation in terms of the underlying physics of the systems. In order to provide evidence of the robustness of our results, we will study several trajectories of a climate models with incorporate observations and compute θ and D_2 for several sub-periods showing that the results are numerically stable. We study the atmospheric circulation over the North Atlantic and focus on a single field that represents its major features: the sea-level pressure (SLP) [35, 36]. Indeed, it has been shown that SLP fields

can be used to study teleconnection patterns as well as storm track activity and atmospheric blocking [37, 38]. The trajectories of our dynamical systems are successions of SLP fields extracted with daily frequency from the ERA-20CM reanalysis project over the period 1900-2010 [39]. The ERA-20CM consists of 10 members ensemble of a (climate) model whose task is to reconstruct at best the 1900-2010 atmospheric dynamics by constraining the model to include the information from available surface observations. Each member of the ERA 20CM is therefore a slightly perturbed reconstruction of the atmospheric dynamics in the past 110 years. The choice of the North Atlantic domain ($80^\circ \text{W} \leq \text{Long.} \leq 50^\circ \text{E}$, $22.5^\circ \text{N} \leq \text{Lat.} \leq 70^\circ \text{N}$) is motivated by the better observational coverage over the region in the first part of the analysis period compared to other regions of the globe [40]. Before presenting the results for D_2 and θ we would like to stress that i) our analysis will only be representative of the North-Atlantic domain and D_2 will be a proxy of the active degrees of freedom of the atmospheric circulation in this area. Therefore, our results cannot be used to estimate the dimension of the full atmospheric climate attractor. ii) Previous results [15, 41, 42] have shown that the estimates obtained for the daily dimensions are robust with respect to the changes in the datasets, resolution of the climate models, and are linearly insensitive to the size of the domain. This gives us confidence on the applicability of the numerical algorithm described in this paper for climate data since it is largely based on those used in [15, 41, 42].

The result for D_2 and θ on the SLP fields of the ERA-20CM ensemble are presented in Figure 2. For each estimate, we fix the reference trajectory x as the first member (M1, for reproducibility) of the ERA-20CM ensemble, while y is alternately set as the i th member with $1 < i < 11$. To test the robustness of the results, we provide four estimates of D_2 and θ : i) using the full data in the period 1900-2010, ii) using 1900-1955 data, iii) using 1900-1928 data and iv) considering only the first 14 years (1900-1914) of data. For each member, the results are reported in Figure 2. The ensemble averages of D_2 and θ for the different periods are instead reported in Table 2. Estimates are consistent for different periods and the value of $D_2 \simeq 9$ found on average, is slightly lower than the estimates of d_H found in [15] (we remind that $D_2 < d_H$). The value of D_2 roughly corresponds to the number of spatial degrees of freedom active in a North-Atlantic SLP field. Indeed, the domain used for this analysis can host about 9 large spatial structures reported between 3-4 extratropical cyclones at time and the same number of anticyclones (see the textbook of Holton [43] for estimates of the typical size of these objects). θ is, in fact, the inverse of the average time the two trajectories x and y cluster together. The value of $\theta = 0.5$ correspond therefore to a contraction of the phase space associated with a timescale between 2 and 3 days. This is the typical decay rate of baroclinic eddies associated to the low pressure systems observed in SLP fields (see again the textbook by Holton [43] for the decay rates). We finally notice that our formula (2.18) gives for the entropy the value $\log 2$.

3.4. Additive noise

In our previous papers [44], [45], [17] we have analyzed the effect of additive noise on the parameters of the extreme value laws. It consists in defining a family of maps $T_\xi = T + \varepsilon \xi$ with ξ a random variable sampled from some distribution \mathbb{G} (we will take here the uniform distribution on some small ball of radius ε around 0). The iteration of the single map T will be now replaced by the concatenation $T_{\xi_n} \circ T_{\xi_{n-1}} \circ \dots \circ T_{\xi_1}$ and the evaluation of an observable computed along this orbit will be given by the probability measure \mathbb{P} which is the product of $\mathbb{G}^{\mathbb{N}}$ with the so-called *stationary measure* μ_S , verifying, for any real measurable bounded function f : $\int f d\mu_S = \int f \circ T_\xi d\mu_S$: see [20] Chapt. 7 for a general introduction to the matter. In the aforementioned papers [44] and [45] we have shown analytically that for dynamical systems perturbed additively the extremal index $\theta = 1$, no matter what the intensity of the noise is. The proof was supported by numerical experiments, using also other kind of noise. The extremal index is a parameter that quantifies the amount of clustering. In our setting clustering happens in presence of invariant sets, which are periodic points in [44] and the diagonal in [17] and in the present paper too. By looking at formula (2.11), we see

that we estimate the proportion of the neighborhood of the invariant set returning to itself; as we argued above and we will stress in the discussion below, that estimate gives information on the rate of backward volume contraction in the unstable direction. The noise destracting these invariants, we expect the extremal index be equal to 1 or quickly approaching 1 when the noise increases. This is confirmed by the numerical experiments reported in Figure 3 where the value of θ is plotted against the intensity of the noise ε for three maps: $3x \bmod 1$ map, the Baker map and the Lozi map. In all cases, indeed $\theta \rightarrow 1$ for large enough noise. However, with respect to the observables discussed in [44], we find some remarkable differences on the intensity of the noise needed to observe changes of the extremal index from the deterministic values: whereas in [44] we observed significant deviation from the deterministic behavior for very small noise intensities ($\varepsilon \geq 10^{-4}$), here we need $\varepsilon \geq 10^{-2}$, i.e. only large noise amplitudes perturb the estimates of D_2 and θ . This difference can be easily explained: in [44], the extremal index was used to explore the local stability at periodic fixed points, where the dynamics is deeply affected even by a small noise. Here, instead, the extremal index tracks a global property that it is stable with respect to small stochastic perturbations. Indeed for the Lozi map, we cannot obtain estimates of θ for noise larger than 0.1 because the dynamics fall out the basin of attraction.

4. DISCUSSION

For higher dimensional maps q_0 is related to the reciprocal of the determinant of the derivative along the expanding direction and therefore the extremal index $1 - q_0$ is a *measure of the rate of phase space contraction for backward iteration*. Although this quantity slightly differs from the entropy, it provides an important piece of information on the dynamics of the system, that can be linked, e.g. to the global predictability and therefore it can be considered as a new indicator of the local instability in chaotic systems. This interpretation together with that on the correlation dimension D_2 could be useful also to analyze times series arising from the evolution of chaotic systems. We first require to define suitably our distance function given a string of data. This could be accomplished using the same techniques as to detect the embedding dimension, namely by replacing the sample of data with delay vectors of variable lengths; we stress that by computing the GEV with those delay vectors will allow to get exactly the embedding dimension. We mean to develop further this approach in a future paper. Finally the computation of the DEI with our observable (2.1) could be helpful purely stochastic sequences for which the extremal index should be 1 from dynamical systems with an underlying chaotic behavior even in presence of small stochastic perturbations. Again, these further applications of our approach with EVT will be the objects of forthcoming investigations.

5. APPENDIX A: NUMERICAL CODE

This appendix contains the MATLAB code for the computation of the correlation dimension D_2 and the extremal index θ for the map $3x \bmod 1$.

```
%Definition of the parameters
%total iterations
timetot=10^6;
%quantile for Peak over threshold
quanti=0.99;
%we compute the correlation dimension over several trajectories
for traj=1:100
%initialization of variables
x1=ones(1,timetot);
```

```

x2=ones(1,timetot);
%We need a pair of trajectories x1 x2. Set the initial condition as random:
x1(1)=rand;
x2(1)=rand;
%This for loop produces the trajectories
for t=2:timetot
    x1(t)=mod(3*x1(t-1),1);
    x2(t)=mod(3*x2(t-1),1);
end
%Apply the logarithm to the distances
logdista=-log(abs(x1(1000:end)-x2(1000:end)));
%Estimates with D2 with the block maxima
blength=1000;
logextr=blockmaxima(logdista,blength);
[tpar tpari]=gevfit(logextr);
d2_GEV(traj)=1/tpar(2);
%Estimates for D2 (Correlation dimension)
theta2(traj)=extremal_Sueveges(logdista,quanti);
end

```

Auxiliary function extremal_Sueveges for the computation of the extremal index:

```

function [theta]=extremal_Sueveges(Y,p)
u=quantile(Y, p);
q=1-p;
Li=find(Y>u);
Ti=diff(Li);
Si=Ti-1;
Nc=length(find(Si>0));
N=length(Ti);
theta=(sum(q.*Si)+N+Nc- sqrt( (sum(q.*Si) +N+Nc).^2 -8*Nc*sum(q.*Si)) )/(2*sum(q.*Si));
end

```

Ausiliary function blockmaxima for the definition of block maxima:

```

function [blockmax] = blockmaxima(x,blocklength)
if length(x)<blocklength;
    blockmax=NaN;
    warning('Series shorter than block sizes')
else
    nblock=fix(length(x)/blocklength);
    blockmax=ones(nblock,1);
    for k=1:nblock
        blockmax(k)=max( x(((k-1)*blocklength+1):(k*blocklength)));
    end
end
end

```

Acknowledgments

SV was supported by the MATH AM-Sud Project Physeco, by the Leverhulme Trust thorough the Network Grant IN-2014-021 and by the project APEX Systèmes dynamiques: Probabilités et Approximation Diophantienne PAD funded by the Région PACA (France). DF was partially supported by the ERC grant A2C2 (No. 338965).

[1] P. Grassberger and I. Procaccia, in *The Theory of Chaotic Attractors* (Springer, 2004), pp. 170–189.

[2] P. Grassberger and I. Procaccia, *Phys. Rev. Lett.* **50**, 346 (1983).

[3] A. Wolf, J. B. Swift, H. L. Swinney, and J. A. Vastano, *Physica D: Nonlinear Phenomena* **16**, 285 (1985).

[4] M. T. Rosenstein, J. J. Collins, and C. J. De Luca, *Physica D: Nonlinear Phenomena* **65**, 117 (1993).

[5] J. Theiler, S. Eubank, A. Longtin, B. Galdrikian, and J. D. Farmer, *Physica D: Nonlinear Phenomena* **58**, 77 (1992).

[6] J.-P. Eckmann and D. Ruelle, *Physica D: Nonlinear Phenomena* **56**, 185 (1992).

[7] H. Kantz and T. Schreiber, *Nonlinear time series analysis*, vol. 7 (Cambridge university press, 2004).

[8] A. Pikovsky and A. Politi, *Lyapunov exponents: a tool to explore complex dynamics* (Cambridge University Press, 2016).

[9] H. Kantz, G. Radons, and H. Yang, *Journal of Physics A: Mathematical and Theoretical* **46**, 254009 (2013).

[10] A. Politi, *Physical Review Letters* **118**, 144101 (2017).

[11] A. C. M. Freitas, J. M. Freitas, and M. Todd, *Probability Theory and Related Fields* **147**, 675 (2010).

[12] D. Faranda, V. Lucarini, G. Turchetti, and S. Vaienti, *J. Stat. Phys.* **145**, 1156 (2011).

[13] D. Faranda and S. Vaienti, *Geophysical Research Letters* **40**, 5782 (2013).

[14] D. Faranda, M. C. Alvarez-Castro, and P. Yiou, *Climate Dynamics* **47**, 3803 (2016).

[15] D. Faranda, G. Messori, and P. Yiou, *Scientific reports* **7**, 41278 (2017).

[16] F. M. E. Pons, G. Messori, M. C. Alvarez-Castro, and D. Faranda, Preprint:hal-01650250 (2017).

[17] D. Faranda, H. Ghoudi, P. Guiraud, and S. Vaienti, arXiv preprint arXiv:1708.00191 (2017).

[18] Y. Pesin and A. Tempelman, *Random and Computational Dynamics* **3**, 137 (1995).

[19] Y. B. Pesin, *Dimension theory in dynamical systems: contemporary views and applications* (University of Chicago Press, 2008).

[20] V. Lucarini, D. Faranda, J. M. Freitas, M. Holland, T. Kuna, M. Nicol, M. Todd, S. Vaienti, et al., *Extremes and recurrence in dynamical systems* (John Wiley & Sons, 2016).

[21] D. Bessis, G. Paladin, G. Turchetti, and S. Vaienti, *Journal of statistical physics* **51**, 109 (1988).

[22] G. Keller, *Equilibrium states in ergodic theory*, vol. 42 (Cambridge university press, 1998).

[23] G. Keller, *Dynamical Systems* **27**, 11 (2012).

[24] G. Keller and C. Liverani, *Journal of Statistical Physics* **135**, 519 (2009).

[25] M. Viana, *Lectures on Lyapunov exponents*, vol. 145 (Cambridge University Press, 2014).

[26] L.-S. Young, *Ergodic theory and dynamical systems* **2**, 109 (1982).

[27] M. Süveges, *Extremes* **10**, 41 (2007).

[28] A. Ferguson and M. Pollicott, *Ergodic Theory and Dynamical Systems* **32**, 961 (2012).

[29] V. Lucarini, D. Faranda, G. Turchetti, and S. Vaienti, *Chaos: An Interdisciplinary Journal of Nonlinear Science* **22**, 023135 (2012).

[30] G. Paladin and S. Vaienti, *Journal of Statistical Physics* **57**, 289 (1989).

[31] J. C. Sprott and G. Rowlands, *International Journal of Bifurcation and Chaos* **11**, 1865 (2001).

[32] K. Simon, *Proceedings of the American Mathematical Society* **125**, 1221 (1997).

[33] G. Baier and M. Klein, *Physics Letters A* **151**, 281 (1990).

[34] H. Richter, *International Journal of Bifurcation and Chaos* **12**, 1371 (2002).

[35] J. W. Hurrell, *Science* **269**, 676 (1995), ISSN 0036-8075, <http://science.sciencemag.org/content/269/5224/676.full.pdf>, URL <http://science.sciencemag.org/content/269/5224/676>.

[36] G. Moore, I. A. Renfrew, and R. S. Pickart, *Journal of Climate* **26**, 2453 (2013).

- [37] J. C. Rogers, *Journal of Climate* **10**, 1635 (1997).
- [38] L. Comas-Bru and F. McDermott, *Quarterly Journal of the Royal Meteorological Society* **140**, 354 (2014).
- [39] H. Hersbach, C. Peubey, A. Simmons, P. Berrisford, P. Poli, and D. Dee, *Quarterly Journal of the Royal Meteorological Society* **141**, 2350 (2015).
- [40] O. Krueger, F. Schenk, F. Feser, and R. Weisse, *Journal of Climate* **26**, 868 (2013).
- [41] D. Rodrigues, M. C. Alvarez-Castro, G. Messori, P. Yiou, Y. Robin, and D. Faranda (2017).
- [42] D. Faranda, G. Messori, M. C. Alvarez-Castro, and P. Yiou, *Nonlinear Processes in Geophysics* **24**, 713 (2017).
- [43] J. R. Holton, *American Journal of Physics* **41**, 752 (1973).
- [44] D. Faranda, J. M. Freitas, V. Lucarini, G. Turchetti, and S. Vaienti, *Nonlinearity* **26**, 2597 (2013).
- [45] H. Aytac, J. Freitas, and S. Vaienti, *Transactions of the American Mathematical Society* **367**, 8229 (2015).
- [46] Actually we got the equality of the right hand side in the limit of large n when the two small corners of S_n become negligible.
- [47] A precise definition consists in taking the \limsup and \liminf of the ratio of the logarithm of (2.7) with $\log(1/r)$.

TABLE I: Estimates of correlation dimension D_2 and dynamical extremal index (DEI) θ obtained with $l = 100$ trajectories, consisting of $n = 10^6$ iterations. Maxima of $\psi(x, y)$ are extracted in block of $m = 1000$ iterations. The quantile for the estimate of the DEI is $\tilde{s} = 0.99$. For the Arnold Cat's map the convergence to theoretical value is lower and the estimates are provided for $\tilde{s} = 0.99999$ and $n = 10^7$.

Map	D_2 (classical)	D_2 (EVT)	θ (from Lyapunov)	θ (EVT)
Bernoulli's Shifts	1	1.00 ± 0.02	0.667	0.668 ± 0.004
Gauss map	1	1.00 ± 0.03	0.773	0.773 ± 0.005
Cantor IFS	0.667	0.64 ± 0.01	0.5	0.502 ± 0.005
Arnold Cat's map	1.987	2.00 ± 0.06	0.51	0.53 ± 0.06
Baker map	1.41	1.46 ± 0.02	0.47	0.49 ± 0.02
Lozi map	1.38	1.39 ± 0.11	0.37	0.37 ± 0.01
Henon map	1.22	1.24 ± 0.03	0.34	0.43 ± 0.01
Solenoid $a = 1/3$	1.6309	1.64 ± 0.04	0.5	0.51 ± 0.01
Solenoid $a = 1/4$	1.5	1.52 ± 0.03	0.5	0.51 ± 0.01

TABLE II: Estimates of correlation dimension D_2 and extremal index θ obtained for daily sea-level pressure maps for four different periods of the ERA-20CM reanalysis. Values represent average over the 9 ensemble members and uncertainty is expressed as the standard deviation of the ensemble mean.

Period	D_2	θ
1900-2010	8.9 ± 0.8	0.48 ± 0.05
1900-1955	8.8 ± 0.7	0.50 ± 0.03
1900-1928	9.4 ± 0.8	0.50 ± 0.02
1900-1914	9.0 ± 1.0	0.50 ± 0.03

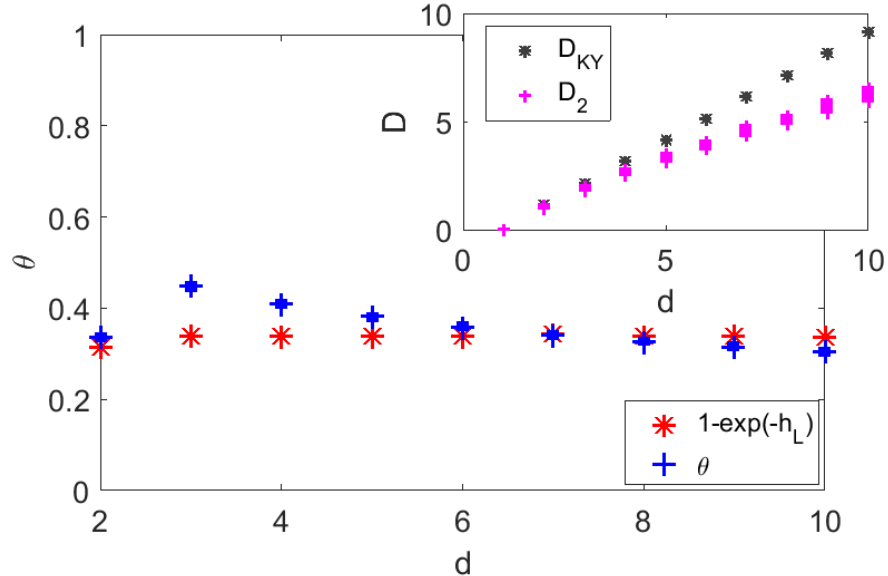


FIG. 1: Estimates of the dynamical extremal index θ and correlation dimension D_2 (inset) obtained for the Generalized Henon maps (Eq. 3.20 in different dimensions d . Values represent the estimates obtained taking 30 couples of trajectories, iterated for $n = 10^6$ iterations. The quantile used for the estimation is $\tilde{s} = 0.98$. Results are compared to those obtained using the Kaplan-Yorke dimension D_{KY} and the entropy h_L . This map has $d - 1$ positive Lyapunov exponents.

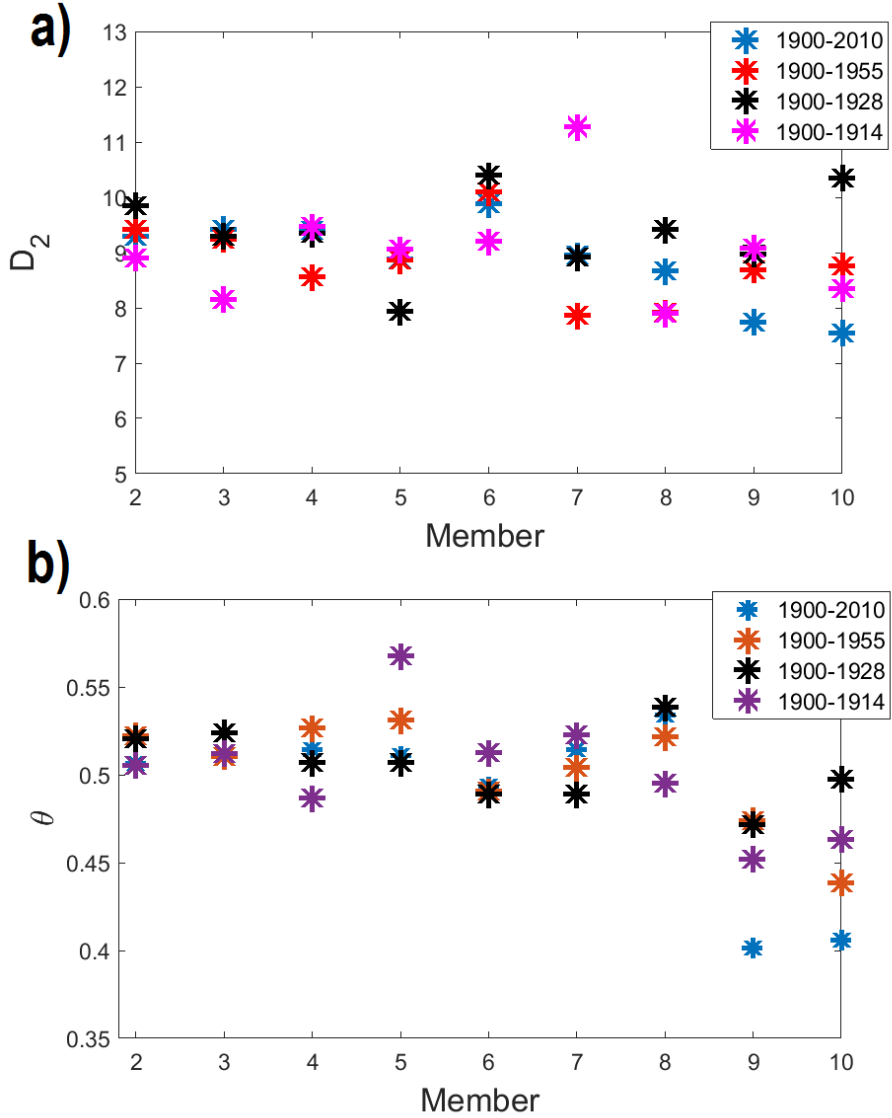


FIG. 2: Estimates of correlation dimension D_2 (a) and extremal index θ (b) obtained for daily sea-level pressure maps for four different periods in the ERA-20CM reanalysis. Values represent the estimates obtained taking as reference trajectory x the member M1 and as y , the remaining 9 ensemble members.

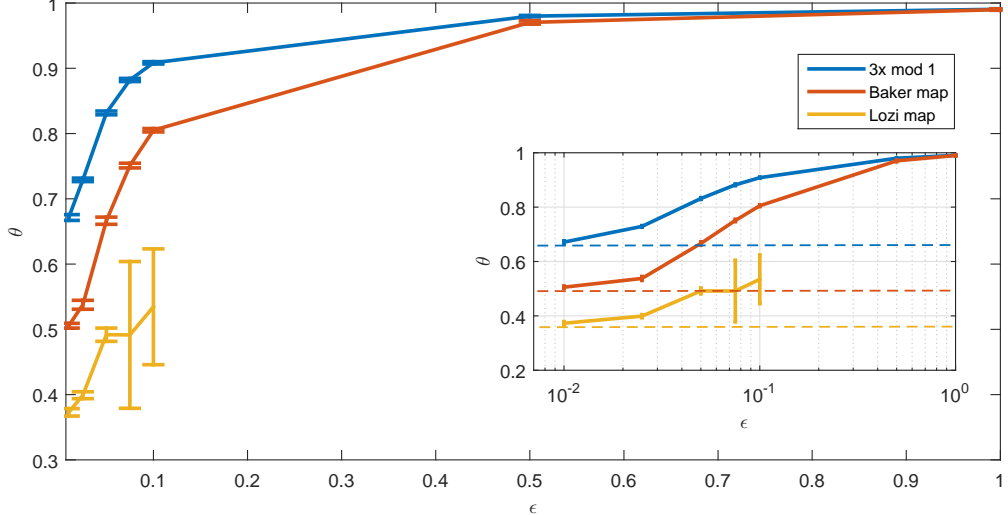


FIG. 3: Dynamical extremal index θ vs intensity of the additive noise ϵ for three different maps: $3x \bmod 1$ (blue), Baker map (red) and Lozi map (orange). The errorbar indicates the standard deviation of the sample of $l = 100$ trajectories, each consisting of $n = 10^6$ iterations. The quantile for the estimate of the extremal index is $\tilde{s} = 0.99$. The inset shows the same data in semilog scale, with the deterministic values represented by dotted lines.